Supplementary Figure 1, Ryba et. al.

A.

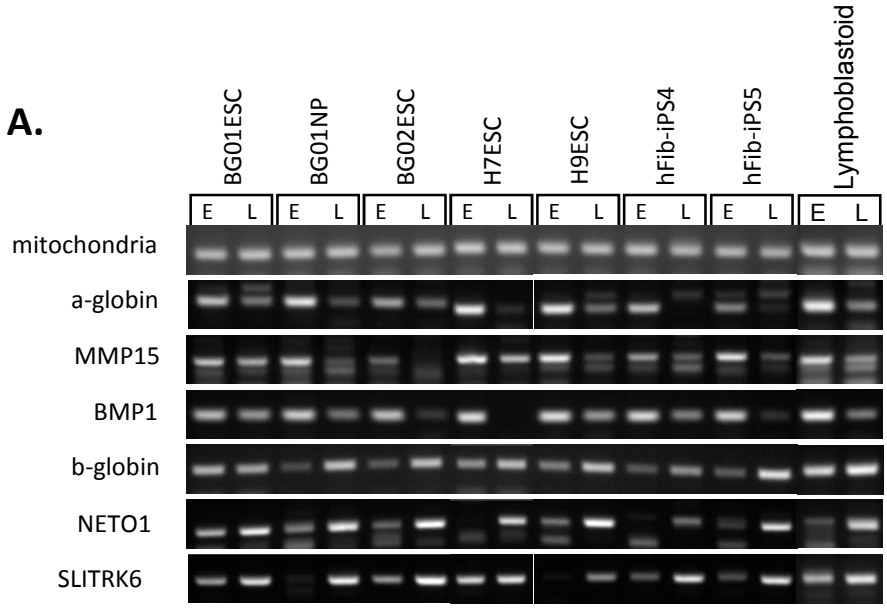

B.

	BG01ESC	BG01NP	BG02ESC	H7ESC	H9ESC	hFib-iPS4	hFib-iPS5	Lymphoblastoid
mitochondria	50%	47%	50%	47%	50%	46%	50%	50%
a-globin	58%	61%	75%	62%	69%	90%	73%	64%
MMP15	55%	64%	66%	56%	71%	59%	73%	56%
BMP1	56%	70%	65%	61%	57%	64%	73%	63%
b-globin	51%	46%	43%	45%	46%	25%	40%	49%
NETO1	43%	37%	41%	37%	38%	19%	31%	22%
SLITRK6	46%	42%	48%	40%	50%	36%	42%	41%

early	>55% early
middle	46-55% early
late	<45% early

Figure S1. Single gene validation of microarray-based replication timing analysis by PCR.
A. Three early replicating markers (α-Globin, MMP15, BMP1) and three late replicating markers (β-Globin, NETO1, SLITRK6) were tested by PCR amplification (in the linear range of the reaction; Hiratani et. al., 2004) of early (E) and late replicating DNA (L) used for microarray hybridization, which showed consistency with microarray data. **B.** Quantification of PCR in A. Percentages of early vs. late-replicating DNA are shown as yellow, gray, or blue for genes replicating early (>55% early), middle (46-55% early) or late (<45% early) in the cell types indicated.

Supplementary Figure 2, Ryba et. al.

A.

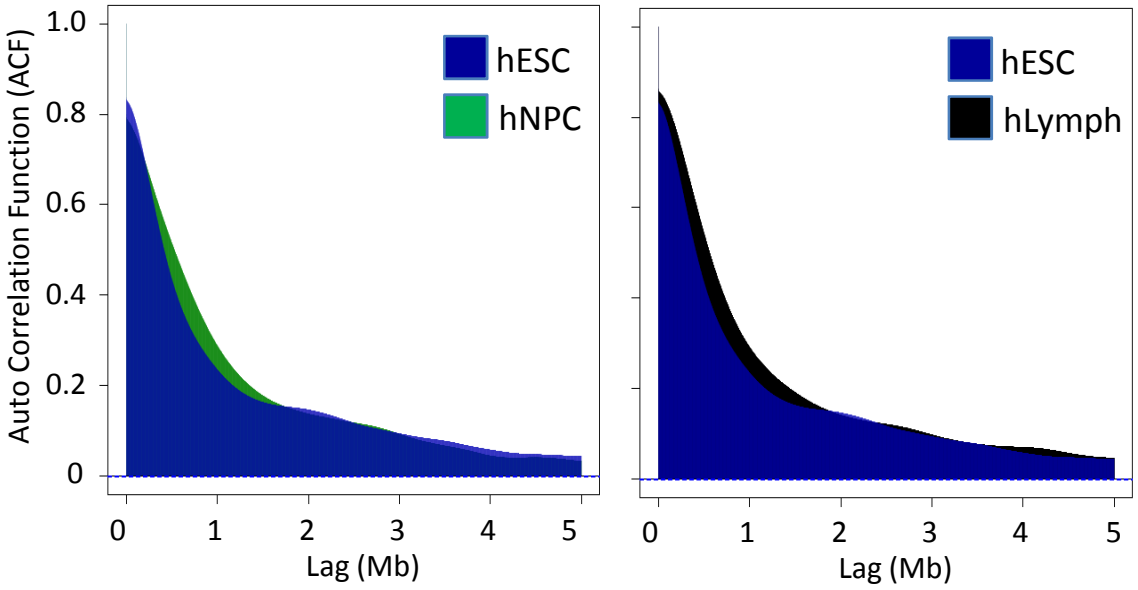

B.

ESC	BG01-R1	BG02-R1	BG02-R2	H7-R2	H9-R1	iPS4-R1	iPS4-R2	iPS5-R1	iPS5-R2
ACF	0.836	0.901	0.719	0.839	0.876	0.701	0.826	0.816	0.754

NPC	BG01-R1	BG01-R2
ACF	0.799	0.870

Lymph	Lymph-R1	Lymph-R2
ACF	0.853	0.793

Averages	BG02 ESC	BG01 NPC	Lymph
ACF	0.862	0.886	0.861

Figure S2. Autocorrelation of neighboring probes. A. Genomewide autocorrelation analysis of replication timing. The autocorrelation function (ACF; y-axis) indicates the average correlation between timing values separated by the indicated genomic distance (Lag; x-axis), and illustrates that similar replication timing values extend over large regions. Lag was calculated using the median probe density of the array. The ACFs for hNPCs (green) and lymphoblast (black) are greater than hESCs (transparent blue overlay) in the 0.5 to 1.7 Mb range, reflecting the larger coordinately replicating regions in these cell types. **B**. Autocorrelations of individual and averaged datasets, with y-values indicated from lag=1kb (nearest probe autocorrelation).

Supplementary Figure 3, Ryba et. al.

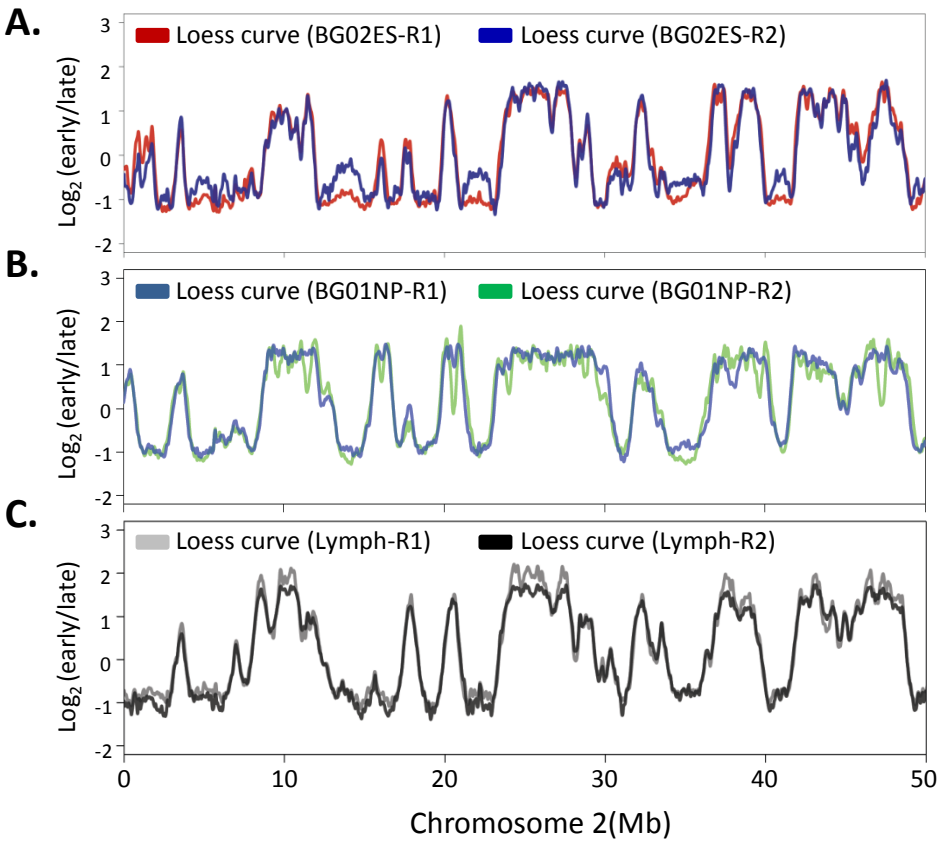

D.

	BG01-R1	BG02-R1	BG02-R2	H7-R1	H9-R1	iPS4-R1	iPS4-R2	iPS5-R1	iPS5-R2
BG01-R1	-								
BG02-R1	0.87	-							
BG02-R2	0.80	0.90	-						
H7-R1	0.88	0.88	0.81	-					
H9-R1	0.86	0.92	0.84	0.89	-				
iPS4-R1	0.88	0.84	0.78	0.89	0.85	-			
iPS4-R2	0.93	0.92	0.86	0.91	0.89	0.94	-		
iPS5-R1	0.89	0.92	0.86	0.89	0.90	0.91	0.90	-	
iPS5-R2	0.89	0.86	0.89	0.88	0.87	0.89	0.89	0.85	-

Figure S3. Conservation of replication profiles within ESCs and between replicates. A,B,C Comparison of loess smoothed replication timing profiles for BG02 ESC (A), BG01 NPC (B), and C0202 lymphoblastoid (C) replicates across a segment of chromosome 2. **D**. Correlations between hESC datasets used in this study, calculated from 300kb loess-smoothed timing profiles as depicted in A-C.

Supplementary Figure 4, Ryba et. al.

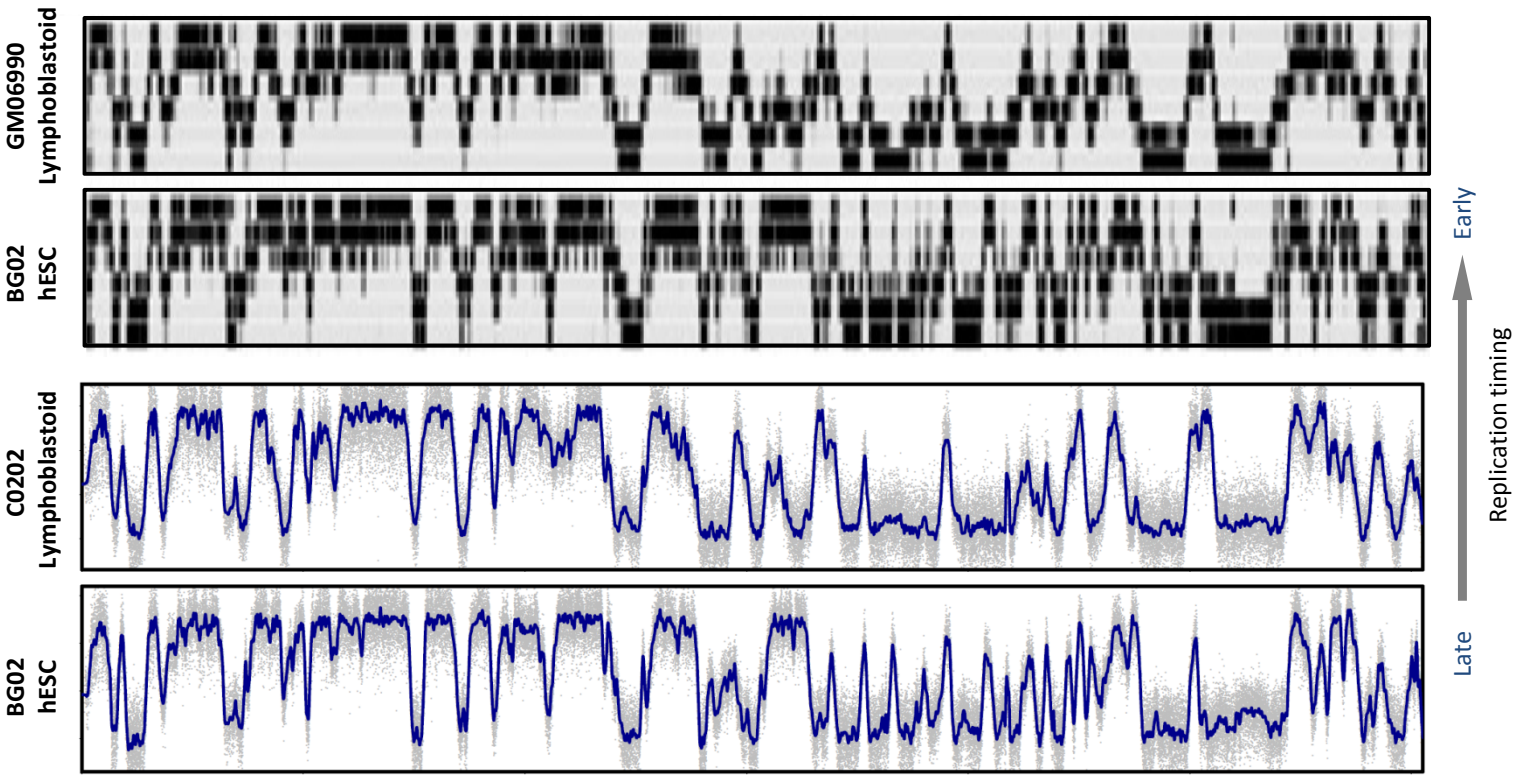

Figure S4. Conservation of replication profiles derived from early/late fractionation and high-throughput sequencing. Repli-Seq timing profiles from Hansen *et al.* 2009 (top) are compared with those from the present study (bottom) along the short arm of chromosome 1. Profiles generated with this method are nearly indistinguishable from profiles created by deep sequencing of similarly prepared BrdU-labeled nascent strands (Hansen *et al*. 2009). Similar results (but with lower signal to noise ratio) are obtained with methods that evaluate S-phase copy number (Hiratani *et al*. 2008; Desprat *et al.* 2009), demonstrating that enrichment for nascent BrdU-substituted strands does not introduce a temporal bias.

We have also shown that microarrays with probe densities from 100 bp to 5.8 kb create almost indistinguishable profiles (Hiratani *et al*. 2008). This is because the minimal BrdU labeling time necessary for reliable immunoprecipitation of nascent strands (1-2 hours) labels >100kb stretches of DNA. Moreover, replication proceeds via nearly synchronous firing of clusters of irregularly spaced replication origins that are utilized heterogeneously in a population of cells (i.e. different cells utilize different cohorts of initiation sites) and together replicate large replication domains in short periods of time. Hence, the resolution of replication timing analyses is limited by the biology of replication, allowing reliable genome-wide replication timing analyses to be rapidly and inexpensively performed on a single oligonucleotide chip.

Supplementary Figure 5, Ryba et. al.

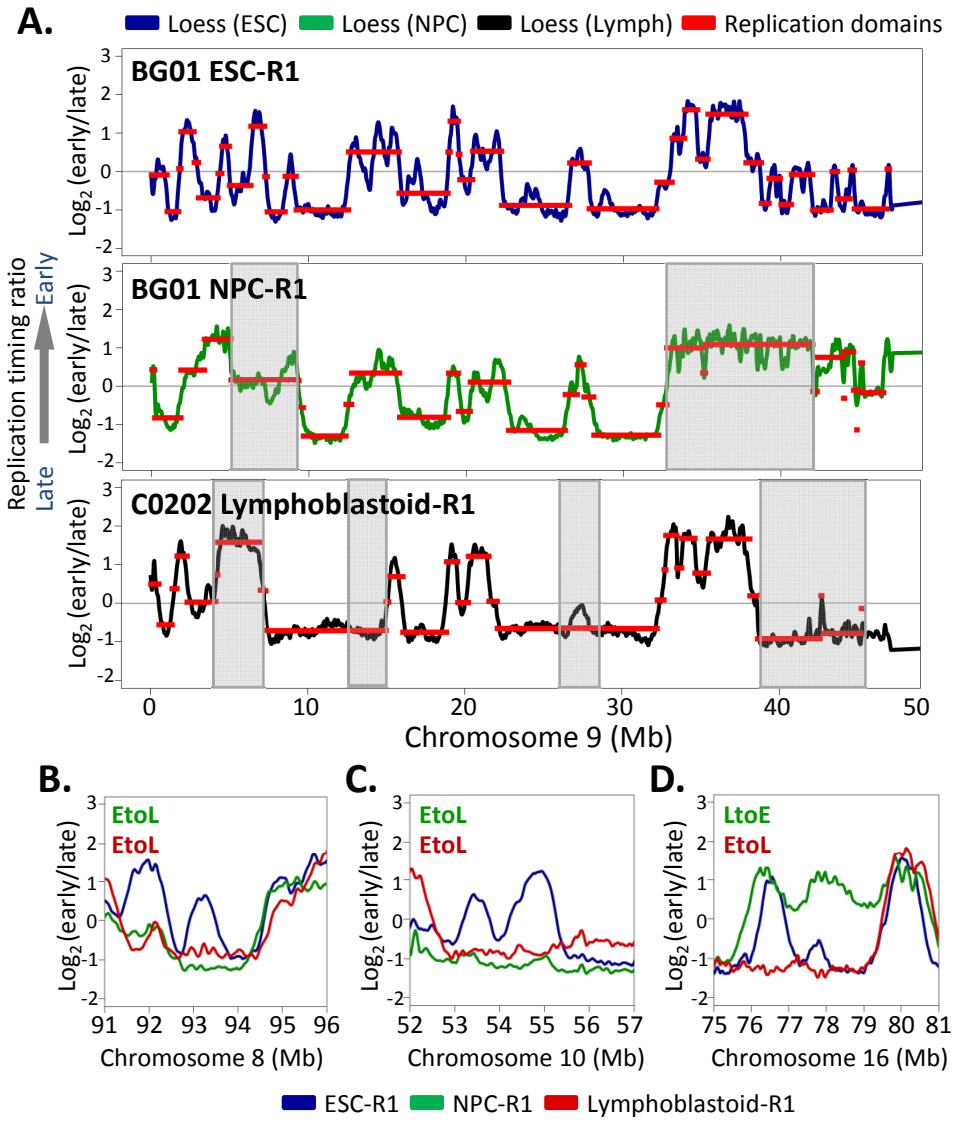

Figure S5. Consolidation of replication timing upon differentiation of hESCs. A. Replication profiles of hESCs, hNPCs, and lymphoblastoid cells across a segment of chromosome 9, illustrating cell type-specific consolidation of domains into fewer and larger units in differentiated cell types. Consolidating regions are highlighted in grey. Genome-wide results are quantified in Figures **2F**, **S6**, and **S7**. **B-D.** Expanded examples of Early-to-Late (EtoL; B-D) and Late-to-Early (LtoE; D) replication domain consolidation.

Supplementary Figure 6, Ryba et. al.

	Mean domain size (Mb)			Consolidation		Mean RT		
Chr	ESC	NPC	Lym	NPC/ESC	Lym/ESC	ESC	NPC	Lym
chr1	1.2	1.6	1.8	**1.3**	**1.5**	0.33	0.25	0.52
chr2	1.4	1.6	1.5	**1.2**	**1.1**	0.01	0.10	0.44
chr3	1.7	1.9	2.0	**1.1**	**1.2**	0.05	0.04	0.44
chr4	1.6	1.9	2.5	**1.2**	**1.6**	-0.14	-0.26	0.34
chr5	1.0	1.3	1.5	**1.3**	**1.5**	0.02	-0.03	0.30
chr6	1.1	1.7	1.6	**1.6**	**1.5**	0.02	-0.02	0.38
chr7	1.1	1.2	1.4	**1.2**	**1.2**	0.18	0.05	0.31
chr8	1.2	1.4	1.6	**1.2**	**1.4**	-0.16	-0.14	0.30
chr9	1.6	1.8	2.2	**1.1**	**1.3**	0.11	0.14	0.41
chr10	1.0	1.7	1.2	**1.6**	**1.2**	-0.08	-0.07	0.38
chr11	1.0	1.5	1.5	**1.5**	**1.5**	0.11	0.15	0.42
chr12	1.0	1.5	1.5	**1.5**	**1.5**	0.13	0.18	0.37
chr13	1.8	1.4	2.0	**0.8**	**1.1**	-0.31	-0.24	0.06
chr14	0.9	1.5	1.4	**1.6**	**1.6**	0.02	0.09	0.32
chr15	1.1	1.3	1.2	**1.2**	**1.1**	0.19	0.27	0.14
chr16	1.1	1.7	1.0	**1.5**	**0.9**	0.07	0.13	0.28
chr17	1.1	1.5	1.4	**1.3**	**1.3**	0.57	0.45	0.43
chr18	1.0	1.3	1.8	**1.3**	**1.8**	-0.38	-0.16	0.01
chr19	1.3	2.7	2.1	**2.0**	**1.6**	0.59	0.24	0.25
chr20	0.9	1.6	1.3	**1.7**	**1.5**	0.02	0.22	0.17
chr21	1.4	1.6	1.6	**1.1**	**1.1**	-0.34	-0.08	0.00
chr22	0.7	1.4	1.6	**1.9**	**2.3**	0.71	0.57	0.25
chrX	1.4	1.9	2.5	**1.4**	**1.8**	-0.04	-0.39	0.13
chrY	3.2	4.8	4.4	**1.5**	**1.4**	-0.52	-0.89	-0.33

Figure S6. Chromosomal replication domain size, consolidation, and average RT in ESCs, NPCs and lymphoblast. The ratios of mean domain sizes in NPCs/ESCs or NPCs/Lymphoblastoid cells (Lym) illustrate the relative levels of consolidation for each chromosome. Chromosomes with earlier (more positive) average replication timing (Mean RT) in mESCs generally undergo greater consolidation.

Supplementary Figure 7, Ryba et. al.

A.

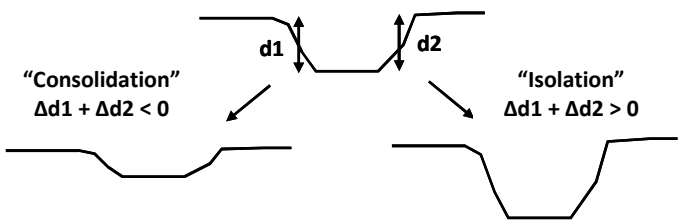

B.

	Number of domains		
	Domains	Consol.	Isol.
All	1545	858 (56%)	687 (44%)
EtoL	78	49 (63%)	29 (37%)
LtoE	78	55 (71%)	23 (29%)

	d1+d2 amount		
	ESC d1+d2	NPC d1+d2	%Change
All	2193.8	1938.9	-11.6
EtoL	80.2	65.9	-17.9
LtoE	60.4	38.6	-36.2

	d1+d2 amount – size weighted		
	ESC d1+d2	NPC d1+d2	%Change
All	4205.8	4412.8	4.9
EtoL	43.7	35.9	-18.0
LtoE	44.3	26.2	-40.8

C.

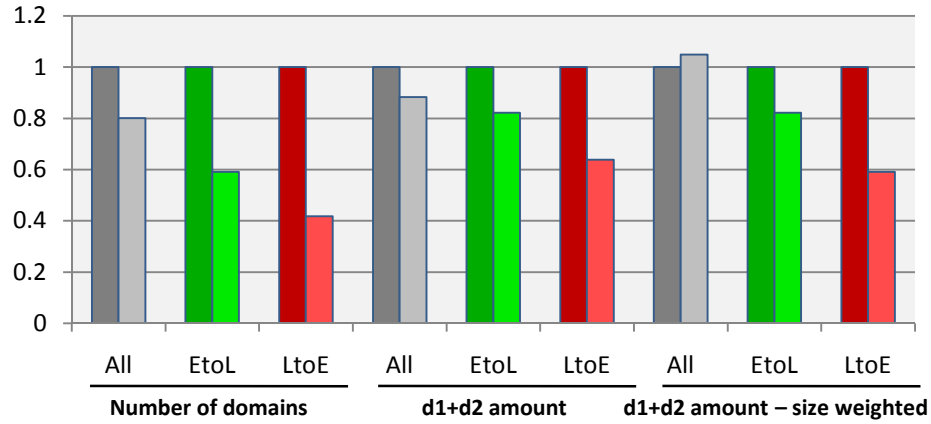

Figure S7. Quantification of domain consolidation. A. Schematic illustration of the definition of "consolidation" or "isolation" used to quantify the degree of such changes occurring during differentiation of hESCs to hNPCs as shown in B. **B.** Quantification of the degree of consolidation vs. isolation for either the total genome (All dRT) or the top 5% EtoL vs. LtoE domain changes during differentiation of hESCs to hNPCs. Tabulated are: the percentage of domains deemed to be consolidating vs. isolating (% of domains); the sum total amount of change in the positive (isolating) or negative (consolidating) direction (d1+d2 amount); the sum total amount (d1+d2) adjusted for the relative fraction of the genome (or sum total size of domains) found in either all domains or the EtoL vs. LtoE switching domains. In all cases, LtoE consolidation is found to be greater than EtoL consolidation. Note that size-weighted results of change for the total genome should theoretically equal zero, since relative earlier changes must equal relative later changes. Hence the 4.9% change provides a reasonable estimate of the error found in these types of calculations and supports the significance of the consolidation seen with EtoL and LtoE domains. **C**. Measures of consolidation (dark bars) vs. isolation (light bars) are shown normalized to the amount of consolidation in each category, demonstrating the greater relative degree of consolidation in LtoE switching domains.

Supplementary Figure 8, Ryba et. al.

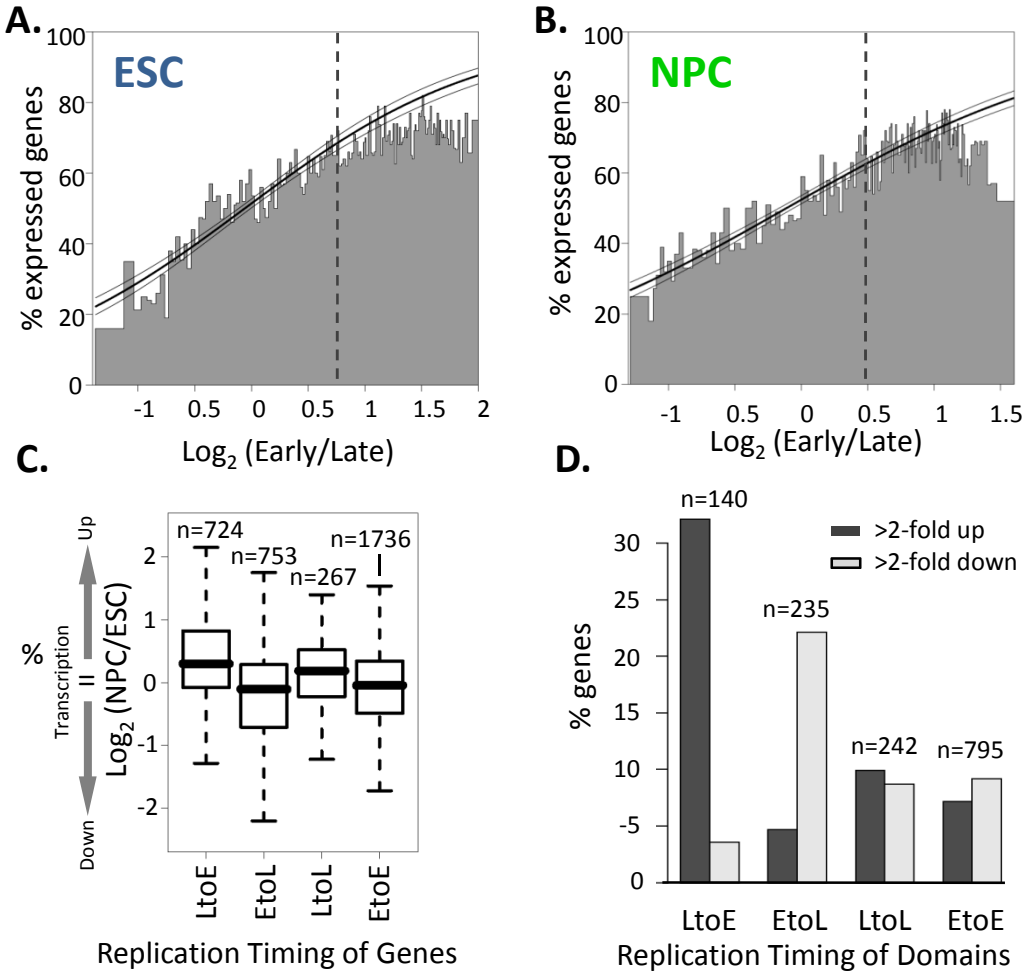

E.

Expression pattern of genes within a domain	LtoE (78)	EtoL (78)	LtoL (41)	EtoE (81)
Up + Unchanged	60%	8%	22%	14%
Down + Unchanged	2%	48%	31%	15%
Up + Down + Unchanged	8%	2%	19%	32%
Unchanged Only	21%	18%	16%	35%
Silent Only (*)	8%	23%	13%	4%

Figure S8. Relationships between replication timing and transcription in hESCs and hNPCs.
Transcription microarray analyses were performed using RNA isolated from aliquots of the same BG01 ESC and NPC cell preparations used for replication timing analyses. **A,B.** Probability of gene expression as a function of replication timing in ESCs (C) and NPCs (D), with each bar representing a bin of 100 genes. Bar heights represent the percentage of expressed genes within each bin, while widths represent the range of replication timing. A dashed line is shown at the median RT value for genes in ESCs and NPCS. Logistic regression (curved line, with outer lines at 95% confidence intervals) was applied. Results are similar to those found in mouse (Hiratani et. al., 2008), including a reduced relationship between gene expression and replication timing for genes replicated in the first half of S-phase (>0.5 RT), which has now been observed in humans, mice and flies (Hiratani, et al., 2009). **C.** Box plots of fold changes in expression [$\log_2$(NPC/ESC] for LtoE, EtoL, LtoL, and EtoE genes. RefSeq genes with the top 5% of RT changes were defined as EtoL and LtoE, while those with the lowest 20% of timing changes that remained above 0.65 or below -0.65 were designated EtoE and LtoL respectively. **D.** Bar plot of the percentage of genes within the boundaries of LtoE, EtoL, LtoL, or EtoE domains (classified as for genes in C) that are >2-fold up- (dark gray) or >2-fold downregulated (light gray). **E.** Summary of >2-fold expression changes within the boundaries of replication domains (classified as in D; numbers in parentheses indicate the number of domains in each class).

Supplementary Figure 9, Ryba et. al.

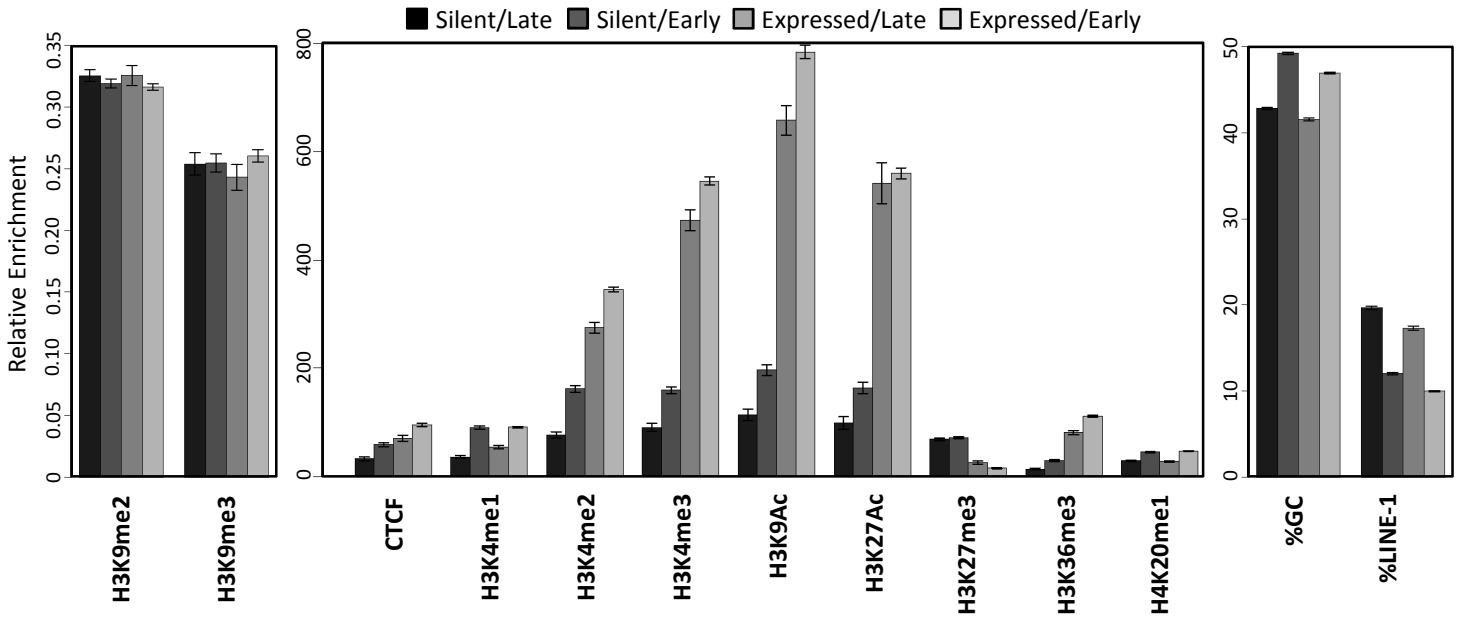

Figure S9. Genetic and epigenetic properties by gene expression and replication timing classes. Relative enrichment of chromatin marks and GC/LINE-1 content are analyzed at the promoters of RefSeq genes. Bars represent averages and standard error of the mean for four categories of genes: silent(<400 expression units)/late(RT value <0), silent/early, expressed/late, and expressed/early. Although significantly correlated with replication timing at a domain level (Figure 4), many chromatin marks (e.g., H3K4me3, H3K9Ac, H3K27Ac, H3K27me3, H3K36me3) are more closely associated with gene expression than replication timing at the level of individual gene promoters. Conversely, local GC and LINE-1 content have a stronger relationship to replication timing than gene expression.

Supplementary Figure 10, Ryba et. al.

A.

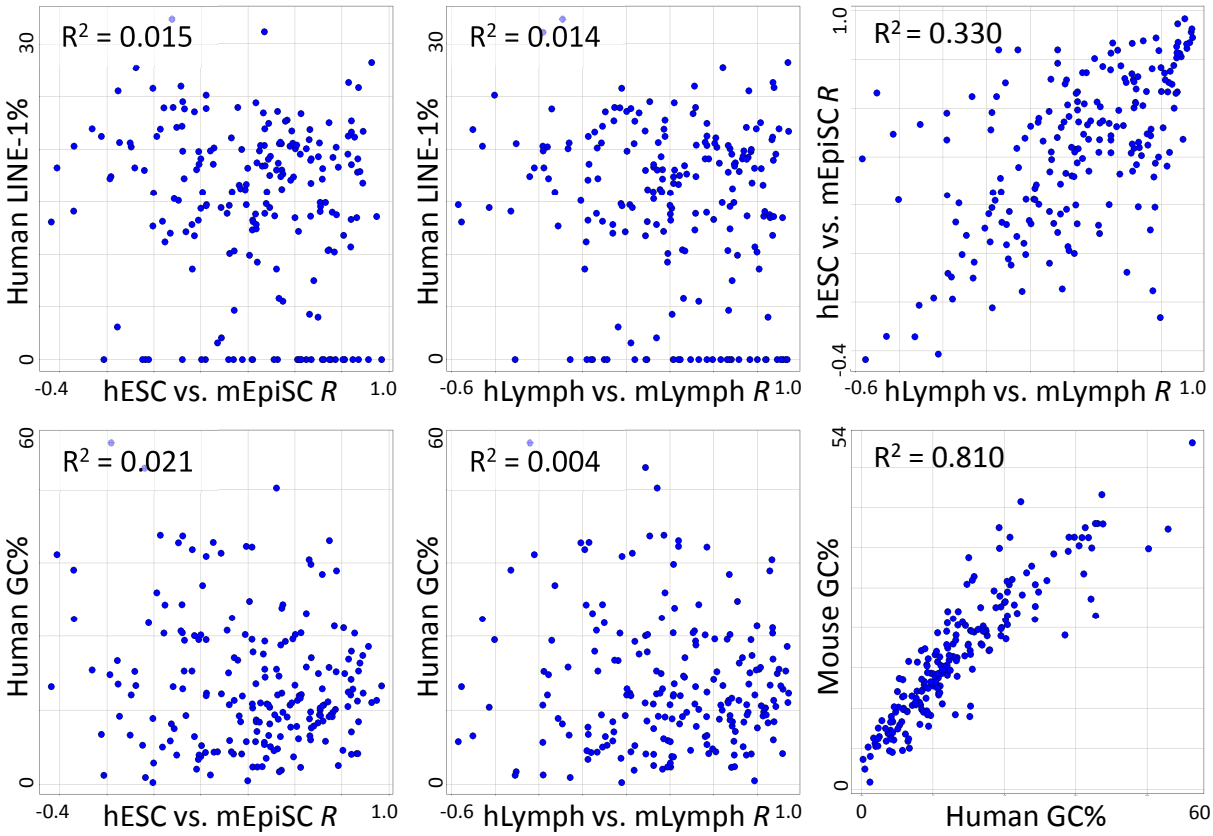

B.

hESC / mEpiSC *R vs:*	
Mark	R^2
Lymph. *R*	**0.330**
NPC *R*	**0.276**
CTCF	0.030
H3K4me1	0.025
H3K4me2	0.030
H3K4me3	0.026
H3K9ac	0.032
H3K27ac	0.014
H3K27me3	0.010
H3K36me3	0.020
H4K20me1	0.021

C.

hLymph / mLymph *R vs:*	
Mark	R^2
hES/mEpi *R*	**0.330**
NPC *R*	**0.248**
CTCF	0.019
H3K4me1	0.043
H3K4me2	0.014
H3K4me3	0.013
H3K9ac	0.010
H3K27ac	0.003
H3K27me3	0.004
H3K36me3	0.022
H4K20me1	0.008

D.

	Size change			
	Relative		Absolute	
R^2 of:	bp	%	bp	%
ESC *R vs:*	0.00	0.03	0.03	0.07*
NPC *R vs:*	0.01	0.04	0.03	0.08*
Lymph *R vs:*	0.02	0.03	0.06*	0.08*

Figure S10. Little relationship between syntenic region RT correlation and levels of genetic and epigenetic marks. **A.** To determine whether differences in RT correlation in individual syntenic regions are related to differences in sequence content, levels of chromatin marks, or overall changes in region size, we compared these properties across the 207 regions of conserved synteny. Neither GC nor LINE-1 content were significantly related to the level of timing conservation; however, average GC content is very well conserved across syntenic regions (lower right panel). **B,C**. Correlation of replication timing across syntenic regions versus levels of epigenetic marks, for human ESC/mouse EpiSC (**B**) or human lymphoblast/mouse lymphoblast (**C**) comparisons. Similarly to sequence properties in **A**, no epigenetic mark was significantly associated with the level of timing conservation, but regions well conserved in one cell type were typically conserved in the other two. **D**. Significant (*) but slight correlations are found between changes in syntenic region size from mouse to human, expressed as absolute or relative (direction preserved) changes in number or percentage of bases in syntenic regions.

Supplementary Figure 11, Ryba et. al.

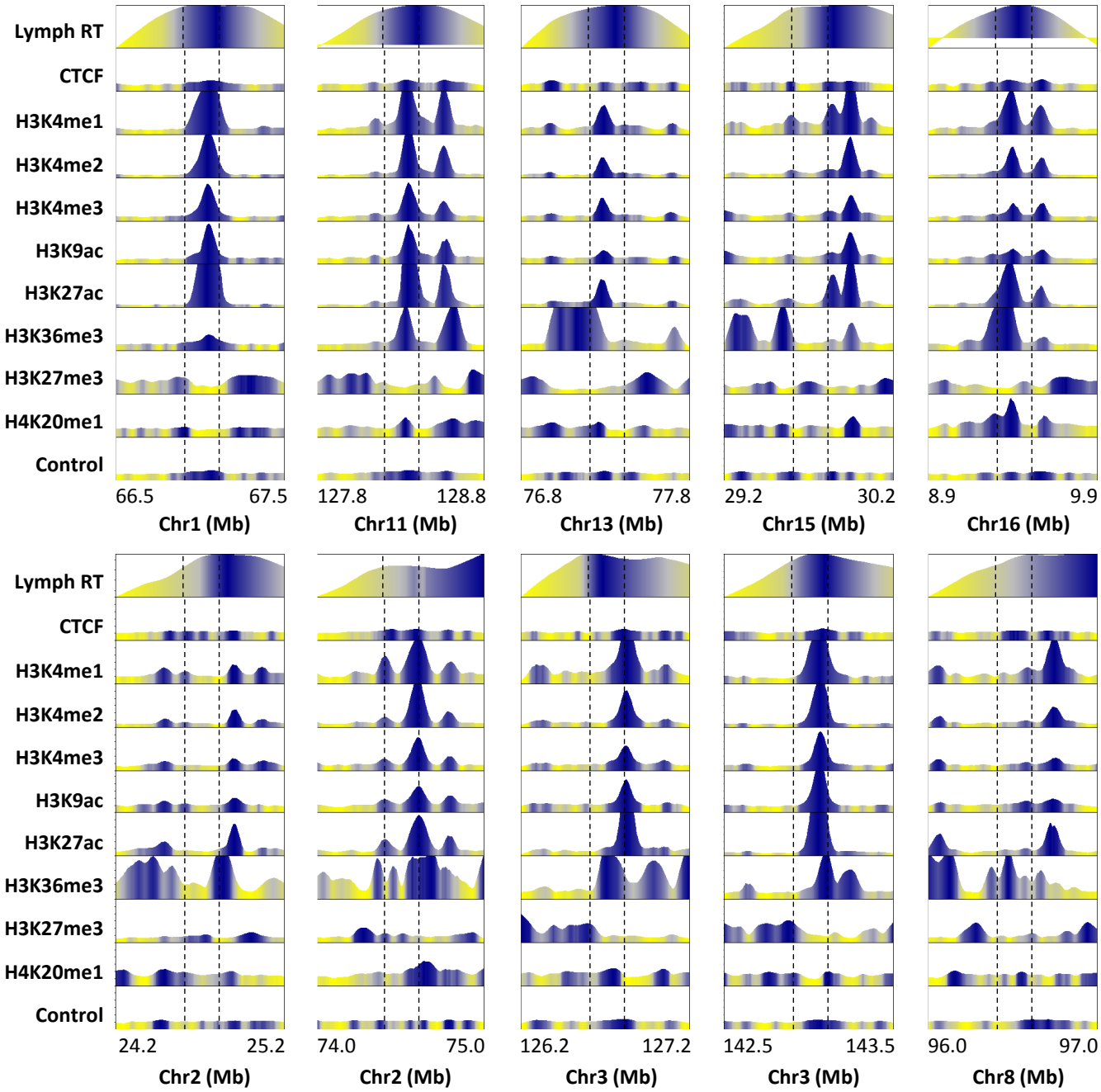

Figure S11. Chromatin marks at the early boundary of individual TTRs. Chromatin marks analyzed as in Figure 5A are examined at the early borders of 10 individual TTRs identified as in Figure 1C, with dashed lines enclosing 200kb (+/- 100kb) from the TTR boundary. Note that peaks of activating marks in somewhat different positions relative to the TTR boundary suggest that the overall peak identified in Figure 5D may be a composite of individual peaks in different locations.